Recent improvements on the atomic fountain clock at SIOM*

Du Yuan-Bo(杜远博)[a)b)], Wei Rong(魏 荣)[a)†], Dong Ri-Chang(董日昌)[a)b)], Zou Fan(邹 凡)[a)b)], and Wang Yu-Zhu(王育竹)[a)]

[a)] *Key Laboratory of Quantum Optics and Center for Cold Atom Physics, Shanghai Institute of Optics and Fine Mechanics, Chinese Academy of Sciences, Shanghai* 201800, *China*

[b)] *University of Chinese Academy of Sciences, Beijing* 100049, *China*

(Received 29 October 2014; revised manuscript received 5 February 2015; published online 29 May 2015)

We report the recent advance in our rubidium atomic fountain clock (AFC). The parameters of the Ramsey cavity are optimized by balancing the coupling from the two ports. The temperature control system of the Ramsey interaction region is renovated, and the resonant temperature of the Ramsey cavity is regulated to be slightly above the room temperature. The quality of magnetic environment in the Ramsey interaction region is also improved. A new digital-to-analog converter (DAC) circuit that controls the local oscillator is adopted to decrease the noise of the oven-controlled crystal oscillator output. As a result, the short-term fractional frequency stability of $2.7\times10^{-13}\tau^{-1/2}$ and the long-term fractional frequency stability of 1.6×10^{-15} at the average time of 32800 s are achieved.

Keywords: atomic fountain clock, Ramsey cavity, frequency stability

PACS: 06.30.Ft, 42.50.–p, 32.30.–r **DOI:** 10.1088/1674-1056/24/7/070601

1. Introduction

The atomic fountain clock is the most accurate frequency standard in the TAI system.[1] At present, the best records of the type-B fractional uncertainty and the long-term frequency stability of the atomic fountain clocks (AFCs) are approximately 1.1×10^{-16}[2] and 6.0×10^{-17} at average time of 10^7 s,[3] respectively. To improve the performance of the AFC, several physical effects, such as second-order Zeeman shift,[4] collision shift,[5] and distributed cavity phase (DCP) shift,[6] that influence the frequency stability and uncertainty of the AFCs, need to be deeply investigated. This is followed by efforts to optimize the corresponding physical parameters for specific effects, which lead to the improvement of the frequency stability and reduction of the uncertainty. Through such process, the type-B uncertainty of the FO1 in the LNE-SYRTE is improved by nearly an order of magnitude.[7,8] This paper presents the latest improvements of our AFC, including reassembly of the physical system, replacement of some components in the AFC, and optimization of physical parameters in the physical system.

In 2005, a rubidium AFC was constructed at the Shanghai Institute of Optics and Fine Mechanics (SIOM). After that, we performed physical experiments like cold atom cloud launch, detection of time of flight (TOF) signal, and Ramsey fringe scanning. Based on the physical experiments above and design of servo loop, we realized the locking of the AFC and preliminarily evaluated the uncertainties of the AFC.[9,10] Before the reassembly of the physical equipment, the short-term frequency stability and the frequency uncertainty are $5.0\times10^{-13}\tau^{-1/2}$ and 2.4×10^{-15}, respectively,[11] which denotes that there is still room for us to improve the performance of our AFC, compared with the most advanced AFCs worldwide. To improve the performance index of our AFC, we reassembled the physical system of the AFC, renovated both Ramsey cavity and temperature control system, and replaced the servo control for the local oscillator.

2. Improvements of the AFC

During the reassembly of our AFC, several improvements were made. The main improvements include: i) adjustment of the Ramsey cavity coupling to balance reflection, ii) reduction in the operating temperature of the Ramsey interaction region, iii) improvement of the magnetic environment in the Ramsey interaction region, and iv) adoption of better servo electronics that control the local oscillator.

2.1. Adjustment of the Ramsey cavity coupling

The previous evaluation result shows that the total uncertainty of our AFC is 2.4×10^{-15}. There are several significant physical effects that influence the uncertainty of our AFC, among which the effect of the microwave power-related shift, including DCP shift and microwave leakage, ranks the first and contributes an uncertainty of 1.8×10^{-15}.[11] Further study shows that the large uncertainty of the microwave power-related shift is ascribed to inappropriate parameter setting of the Ramsey cavity (the cavity geometry diagram is illustrated in Fig. 1(a)). To measure the parameters of the Ramsey cabitly, the return loss of the Ramsey cavity in the two ports was measured by a network analyzer. As presented in Fig. 1(b), the difference of return loss between the two ports of the Ramsey cavity reaches 2.5 dB in the peak and sideband.

*Project supported by the National Natural Science Foundation of China (Grant Nos. 61275204 and 91336105).

†Corresponding author. E-mail: weirong@siom.ac.cn

© 2015 Chinese Physical Society and IOP Publishing Ltd

The coupling unbalance from the two ports will induce microwave field oscillating in a horizontal mode in the axial direction, leading to unwanted $\Delta F = 1$ and $\Delta m_{\rm F} = \pm 1$ magnetic dipole transition.

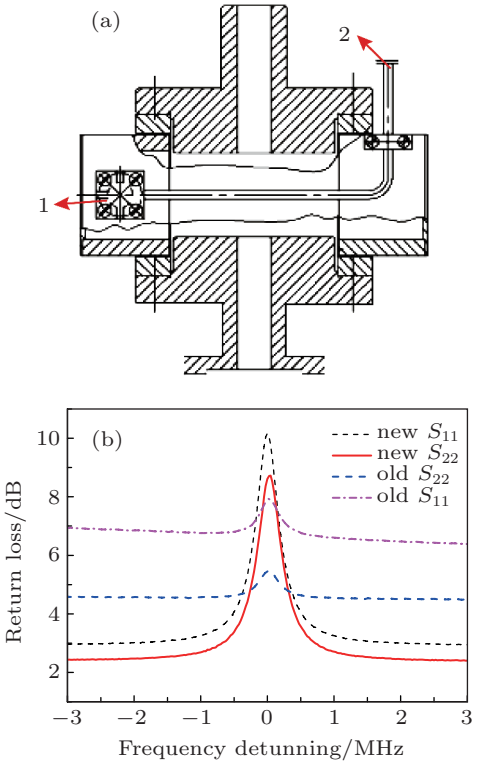


Fig. 1. (color online) (a) Geometry diagrams of the Ramsey cavity, where labels 1 and 2 indicate the two microwave coupling ports. (b) The measured reflection curve S_{11} and S_{22} of the Ramsey cavity, which denotes the return loss before (dot: S_{11}, dash dot: S_{22}) and after the improvement (dashed line: S_{11}, solid line: S_{22}).

To reduce the uncertainty of power-related shift, we renovated components of the Ramsey cavity, and adjusted the corresponding parameters of the Ramsey cavity. The two waveguide tubes were remade, a tuning screw was inserted in each side of the waveguide to tune the capacitive character of the Ramsey cavity, and the positions of the antennae connected to the two waveguide tubes were adjusted to realize the optimal coupling of microwave. In addition, to avoid microwave leakage, an indium wire was used to seal the aperture between the rectangle waveguide and the cylindrical cavity. By these adjustments, the difference of return loss between the two ports of the Ramsey cavity is reduced to 1.5 dB in the peak and 0.5 dB in the sideband, as shown in Fig. 1(b), which signifies that the microwave coupling has been optimized. According to Refs. [6] and [12], it is expected that the uncertainty caused by the microwave power-related shift be reduced to less than 1.0×10^{-15}.

2.2. Temperature control system in the Ramsey interaction region

The blackbody radiation (BBR) shift at a certain temperature T could be written as[13]

$$y_{\rm BBR} = \beta \left(\frac{T}{T_0}\right)^4 \times \left[1 + \varepsilon \left(\frac{T}{T_0}\right)^2\right], \quad (1)$$

where T_0 is 300 K, $\beta_{\rm Rb} = -1.256(13) \times 10^{-14}$, and $\varepsilon_{\rm Rb} = 0.011(1)$ for ^{87}Rb.[14] The operating temperature in the Ramsey interaction region of the AFC is decided by the resonant frequency of Ramsey cavity which should be tuned to be coincident with the transition frequency of the ^{87}Rb AFC. The operating temperature is usually set a little higher than the room temperature to facilitate the active control or adiabatically follow the room temperature. The previous temperature in our AFC was set to 53.2 °C, which leads to a large temperature difference between the inner region and the ambient environment (25 ± 1 °C), accompanied by a large temperature gradient along the axial direction in the vacuum chamber. In addition, given a same temperature fluctuation, a higher temperature causes a larger uncertainty of BBR shift.[15]

To decrease the operating temperature and the temperature gradient, we rubbed the surface of the end cap of the Ramsey cavity to increase the cavity depth and ultimately adjusted the temperature to 29.0 °C. Figure 2(a) shows the physical apparatus of the vacuum chamber in the Ramsey interaction region, evenly adhered by four temperature probes along the vacuum wall, together with the twinning carbon fibers (see Section 2.3). The monitored values of temperature by the four temperature probes indicate that the maximum temperature gradient along the vacuum chamber is decreased from 2.31 °C to 0.97 ° C while the fluctuation (1σ) is reduced from 0.04 °C to 0.02 °C, as shown in Table 1. As a result, the evaluation value of the BBR shift is optimized from $-17.3(2) \times 10^{-15}$ to $-13.0(1) \times 10^{-15}$.

Table 1. The monitored values of temperature (unit: °C) by the four probes which lies on the exterior wall of the vacuum chamber (the standard deviations of certain values are not given for the corresponding probe connected to the exterior temperature control system).

Probe No.	Previous value	Present value
1	51.85(3)	28.07(1)
2	53.2	28.65(2)
3	54.16(3)	29.0
4	53.46(4)	28.30(2)

2.3. Magnetic environment in the Ramsey interaction region

Previously, the temperature of the vacuum chamber in the Ramsey interaction region was maintained by heating stripe made of nickel and zirconium wire, which might induce residual magnetic field when experiencing persistent heating. Thus we adopted the carbon fiber instead of the wire, to eliminate the residual magnetic field, and the physical apparatus diagram of the fiber twinning around the vacuum chamber is illustrated in Fig. 2(a).

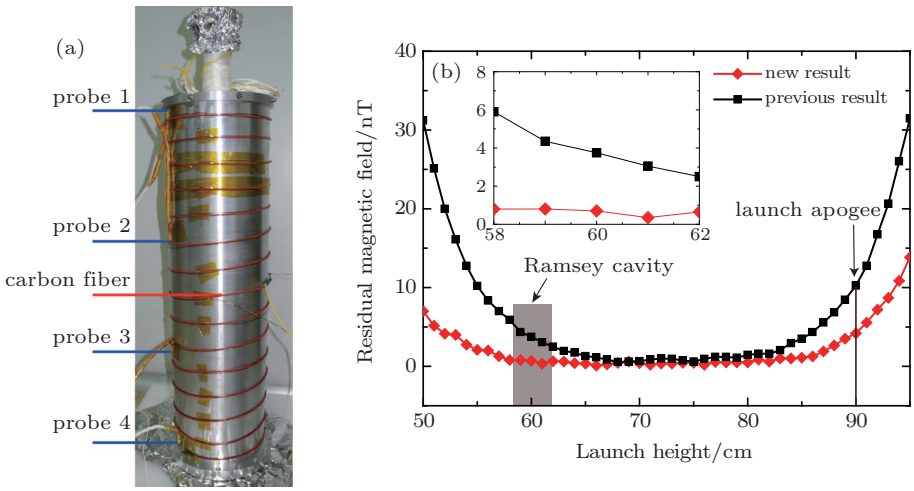


Fig. 2. (color online) (a) The physical apparatus diagram of the vacuum chamber in the Ramsey interaction region of the AFC, together with four temperature probes (lists: 1, 2, 3, 4) and twinning carbon fiber adhered to it. (b) The strength of magnetic field measured along the axial direction in the magnetic shielding cylinder after demagnetizing; the inserted figure illustrates the magnetic distribution in the Ramsey interrogation region (black square: previous value in 2005, red diamond: new result).

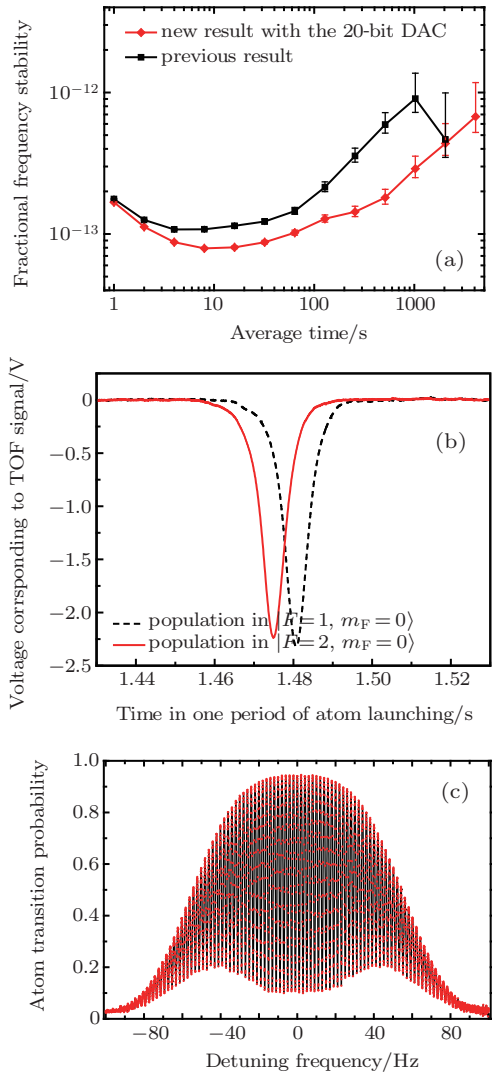


Fig. 3. (color online) (a) The short-term frequency stability of the OCXO versus the H-maser for a given constant control voltage, which shows the control noise of the electronic circuit is reduced. Black square: previous value; red diamond: new result. (b) TOF signal of ^{87}Rb cold atoms populated in $|F=1;m_F=0\rangle$ (dashed line) and $|F=2;m_F=0\rangle$ (solid line) detected in the probe region during the ballistic flight with the temperature of 2.0 μK. (c) The Ramsey fringe measured in the AFC, with the linewidth of 1 Hz and the SNR of 246.

During the reassembly process, we carefully optimized the magnetic environment in the Ramsey interaction region. After demagnetization of the magnetic shielding cylinders composed of four layers of Permalloy, the magnetic distribution along the symmetry axis of the magnetic shielding cylinders was measured, as presented by red diamond of Fig. 2(b). Compared with the previous magnetic distribution in the Ramsey interaction region, there is a smaller residual magnetic field after the improvement. Specially, the average residual magnetic field inside the Ramsey interrogation region is decreased from 3 nT (black square in Fig. 2(b), first installation of the physical system in 2005) to less than 1 nT (red diamond in Fig. 2(b)). The magnetic improvement in the Ramsey interaction region contributes to reduction of the uncertainty caused by second Zeeman shift[4] and Majorana transitions.[16]

2.4. Servo electronics of the local oscillator

The frequency stability of the AFC is limited by noise of the local oscillator and the Dick effect.[17] Compared with the normal locking mode of the AFC in which a DDS in the synthesizer chain records the error signal, the local oscillator (OCXO, Oscilloquartz Corp. BVA-8607) in our AFC is locked by a digital phase lock loop to provide a standard frequency signal. In this locking mode, the control noise from the loop adds to the noise of the local oscillator output, which degenerates the frequency stability of the AFC. Lately, a 20-bit DAC circuit was made to replace the previous servo electronics (voltage resolution of 20 μV) in the loop to control the local oscillator, because it has the advantages of lower noise, higher resolution (7.8 μV), and lower temperature drift (less than 1 ppm/°C). For a constant control voltage, the short-term stability of the local oscillator output noise is measured and shown in Fig. 3(a) (red diamond). The result manifests that the frequency stability of the local oscillator is improved compared with the previous result (black square in Fig. 3(a)).

Lower noise in the local oscillator leads to the improvement on the stability of the AFC.

2.5. Experiment results after the reassembly

Besides the main improvements mentioned above, we optimized the vacuum degree of the vacuum chamber from 2.0×10^{-7} Pa to 6.0×10^{-8} Pa after handling of the vacuum system. In general, the improvements lead to optimization of specific parameters in the physical system, as summarized in Table 2. After the reassembly of the physical system, the previous physical experiments were repeated. The TOF signals of atoms populated in $|F=1,m_F=0\rangle$ and $|F=2,m_F=0\rangle$ are detected in the probe region during the ballistic flight (Fig. 3(b)). As shown in Fig. 3(b), the atom temperature is 2.0 μK, which is improved with respect to the previous value of 2.6 μK and the TOF signal also increases by 20%. These improvements are attributed to the vacuum promotion and enhanced compensation of the geomagnetic magnetic field in the magnetic optical trap area.

Table 2. Summary of specific parameters of the physical system before and after reassembly.

Improvement items	Before	After
Cavity resonant temperature control/°C	53.2	29.0
Difference in microwave return loss/dB	Peak: 2.5	Peak: 1.5
Residual magnetic in the interrogation region/nT	3	<1
Vacuum degree/Pa	2.0×10^{-7}	6.0×10^{-8}

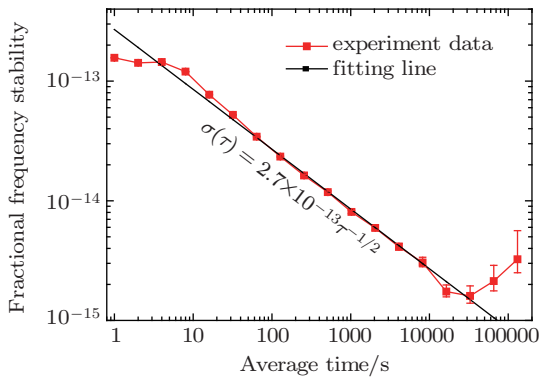


Fig. 4. (color online) Short-term frequency stability of the AFC compared with the H-maser, with the fitting curve $2.7\times10^{-13}\tau^{-1/2}$, and it reaches 1.6×10^{-15} at the average time of 32800 seconds.

It is illustrated in Fig. 3(c) that the Ramsey fringe has a line width of 1 Hz and a signal-to-noise ratio (SNR) of 246. Based on the physical experiments and design of the servo loop, we lock the AFC. The curve of the short-term frequency stability measured with a local H-maser (VCH-1003a, 2×10^{-15}@a day) is presented in Fig. 4. The short-term stability of the comparison data is $2.7\times10^{-13}\tau^{-1/2}$, which reaches 1.6×10^{-15} at an average time of 32800 s. The short-term stability is close to the stability of $2.0\times10^{-13}\tau^{-1/2}$ of the AFC in the USNO,[3] while the long-term stability of the comparison data is limited by the attribute of a significant frequency drift in the H-maser, which results in the deviation of the fitting line at the average time longer than 40000 s. The more precise measurement of the frequency stability of our AFC requires the introduction of another precise frequency standard. We are in the process of evaluating the frequency shift and uncertainty of our AFC.

3. Conclusions

We optimized the microwave coupling in the Ramsey interrogation region, upgraded the temperature control system in the Ramsey interaction region, and improved the vacuum environment. The residual magnetic field inside the magnetic shielding cylinders is also decreased. A new DAC circuit that controls the local oscillator ensures low noise in the microwave synthesizer chain. After the improvements, the frequency stability of the atomic fountain is $2.7\times10^{-13}\tau^{-1/2}$, which reaches 1.6×10^{-15} at an average time of 32800 s. This work lays the foundation for accuracy evaluation of our AFC.

Acknowledgment

We thank Prof. Yuanci Gao for the assistant in the simulation of the cavity configuration and calculation of the optimal parameter of the Ramsey cavity.

References

[1] Bureau International Des Poids Et Meaures 2013 *BIPM Annual Report on Time Activities* (Pavillon de Breteuil)
[2] Heavner T P, Donley E A, Levi F, Costanzo G, Parker T E, Shirley J H, Ashby N, Barlow S and Jefferts S R 2014 *Metrologia* **51** 174
[3] Peil S, Hanssen J L, Swanson T B, Taylor J and Ekstrom C R 2014 *Metrologia* **51** 263
[4] Jefferts S R, Shirley J, Parker T E, Heavner T P, Meekhof D M, Nelson C, Levi F, Costanzo G, Marchi A D, Drullinger R, Hollberg L, Lee W D and Walls F L 2002 *Metrologia* **39** 321
[5] Fertig C and Gibble K 2000 *Phys. Rev. Lett.* **85** 1622
[6] Guéna J, and Li R X, Gibble K, Bize S and Clairon A 2011 *Phys. Rev. Lett.* **106** 130801
[7] Zhang S G 2004 *Déplacement de fréquence dû au rayonnement du corps noir dans une fontaine atomique à césium et amélioration des performances de l'horloge*
[8] Clairon A, Laurent P, Santarelli G, Ghezali S, Lea S N and Bahoura M 1995 *Instrumentation and Measurement, IEEE Transactions on* **44** 128
[9] Shi C Y, Wei R, Zhou Z C, Li T, Li L and Wang Y Z 2011 *Frequency Control and the European Frequency and Time Forum (FCS), 2011 Joint Conference of the IEEE International*
[10] Wei R, Zhou Z C, Shi C Y, Zhao J B, Li T and Wang Y Z 2011 *Chin. Phys. B* **20** 089501
[11] Du Y B, Wei R, Dong R C and Wang Y Z 2013 *China Satellite Navigation Conference 2013 Proceedings* (Berlin: Springer)
[12] Weyers S, Schroder R and Wynands R 2006 *Frequency and Time Forum, 20th European. IEEE*
[13] Itano W M, Lewis L and Wineland D 1982 *Phys. Rev. A* **25** 1233
[14] Angstmann E J, Dzuba V A and Flambaum V V 2006 *Phys. Rev. A* **74** 023405
[15] Jefferts S R, Heavner T P, Parker T E, Shirley J H, Donley E A, Ashby N, Levi F, Calonico D and Costanzo G A 2014 *Phys. Rev. Lett.* **112** 050801
[16] Vanier J and Audoin C 1989 *The Quantum Physics of Atomic Frequency Standards* (Bristol/Philadelphia: Adam Hilger) p. 836
[17] Dick G J 1987 *Local Oscillator Induced Instabilities in Trapped Ion Frequency Standards* (DTIC Document)